JOURNAL OF GEOPHYSICAL RESEARCH, VOL. 113, C12008, doi:10.1029/2008JC004760, 2008

Comment on "Seasonal heat budgets of the Red and Black seas" by Matsoukas et al.

A. B. Kara[1] and C. N. Barron[1]

Received 2 February 2008; revised 9 September 2008; accepted 6 October 2008; published 13 December 2008.

Citation: Kara, A. B., and C. N. Barron (2008), Comment on ''Seasonal heat budgets of the Red and Black seas'' by Matsoukas et al., *J. Geophys. Res.*, *113*, C12008, doi:10.1029/2008JC004760.

1. Motivation

[1] *Matsoukas et al.* [2007] present a monthly analysis of heat fluxes in relation to heat budget in the Red and Black Seas to provide further insight for air-sea exchange processes in the small ocean basins. Components of net surface heat flux are illustrated during 1984–1995. In computing latent and sensible heat fluxes, *Matsoukas et al.* [2007] apply traditional bulk formulations. A heat balance method that is based on the available energy for evaporation flux is also presented to compare latent heat fluxes with those from the bulk formulations. All near-surface atmospheric variables, including wind speed at 10 m, used in the heat balance method are obtained from reanalysis of a numerical weather product (NWP). Initial input data for radiation flux calculations are at resolutions of 1.0° and 2.5°, depending on the availability. Monthly means of heat budget components are computed on the basis of monthly means of atmospheric variables during 1984–2000.

[2] Concerning heat fluxes in the Red and Black Seas, all computations and their details are generally properly presented by *Matsoukas et al.* [2007]. We worry, however, about one major concern (section 3 and 4). We also identify two other potentially important issues and suggest how these might alter results (section 5). Here our major focus is that *Matsoukas et al.* [2007] do not consider the representativeness errors inherent in using input data from a coarse resolution NWP product in studying air-sea exchange processes in small ocean basins, such as the Red and Black Seas. This neglection poses serious errors in heat budget computations. For example, the Red Sea is a narrow inland water body which has relatively shallow water depths (Figure 1). It is roughly 1900 km long and, at its widest point, over 300 km wide. Oceanic features are greatly influenced by seasonally reversing winds in this small region so interactions between the ocean shelf and the adjacent continent are of great interest. Therefore, wind speed at 10 m is expected have great influence on latent and sensible heat fluxes especially near coastlines. Use of improper winds for heat flux computations can thus misleadingly influence heat budget estimates as will be described in section 3. In addition, the 2.5° resolution study used in their data cannot accurately represent sea-only radiative fluxes for the small Red and Black Seas.

2. Resolution of Input Data

[3] The data for surface atmospheric variables in calculating sensible and latent heat fluxes in the paper by *Matsoukas et al.* [2007] are obtained from a NWP product, namely, European Centre for Medium-Range Weather Forecasts. Unfortunately, the gridded global fields provided by the NWP centers are generally at a spatial scale too coarse to appropriately define the contrast between water and land grid points for small ocean basins, such as the Red and Black Seas. Such NWP products are given in Table 1.

[4] Our focus will be on quantifying the accuracy of the wind speed at 10 m from coarse resolution NWP products, including European Centre for Medium-Range Weather Forecasts 40-year Reanalysis (ERA-40) as used by *Matsoukas et al.* [2007]. We particularly use wind speed at 10 m for such evaluations since accuracy of latent and sensible heat flux computations strongly depends on accuracy of winds in the bulk parameterizations. For validations of NWP winds a relatively finer gridded wind product, Quick Scatterometer (QSCAT), is formed from satellite measurements (Table 1). In particular, twice-daily QSCAT wind measurements are obtained from Remote Sensor Systems (RSS), http://www.remss.com, and monthly means of rain-free winds are formed. Data for NWP products are obtained from the National Center for Atmospheric Research (NCAR) data support section (http://dss.ucar.edu/datasets/), and monthly means are constructed using 6 hourly values.

3. Evaluation of ERA-40 Winds

[5] Several problems arise when using wind speed from the 1.125° × 1.125° resolution (≈125 km) ERA-40 product in computing latent and sensible heat fluxes in the Red Sea especially near the coastal boundaries. At best there can be no more than two grid points in the horizontal direction (Figure 1). *Matsoukas et al.* [2007] use a 1° grid resolution, and for a specific latitude, the longitude span was between 1 and 3 grid points for the Red Sea. In any case, winds at most grid points near the land-sea boundaries over the sea are contaminated by land values due to relatively coarse resolution, i.e., a grid point includes wind

[1]Oceanography Division, Naval Research Laboratory, Stennis Space Center, Mississippi, USA.

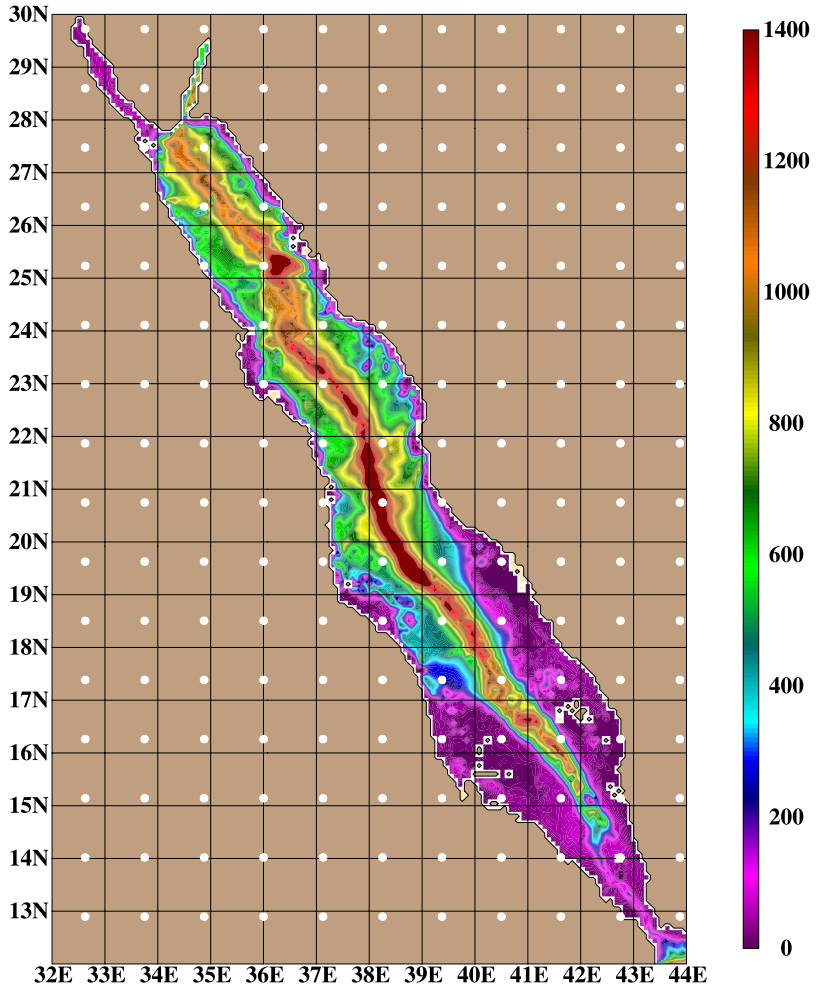

Figure 1. Grid points from the 1.125° resolution ERA-40 shown in filled white circles overlayed on the bottom depth (in m) in the Red Sea. Grid points over the land are also provided. Note that ERA-40 data are distributed on a N80 Gaussian grid, so grid points in the meridional direction deviate from a constant 1.125° resolution. Bottom depths are obtained from the Naval Research Laboratory Digital Bathymetry Database bathymetry database, which has a resolution of 2 minutes (data are available at http://www7320.nrlssc.navy.mil/DBDB2_WWW/).

values from both land and ocean, affecting the accuracy of the computed latent and sensible heat fluxes.

3.1. Land-Sea Mask for NWP Products

[6] The land-sea mask values from all NWP products, including the 1.125° resolution ERA-40 on the Gaussian grid, are interpolated to a finer grid of 1/12° (Figure 2a). This is done in order to demonstrate land contamination of winds near the coastal regions and also their accuracies in the interior. The ocean and land areas in NWP products are typically defined by a land-sea mask of zeros and ones, indicating that a grid cell is treated as all sea or all land, respectively. A percentage land-sea mask value of 40 (100), for example, in Figure 2 explains that wind speed at 10 m

Table 1. Abbreviations and Grid Resolutions for Wind Products Used Throughout the Text[a]

Acronym	Name of Product	Grid Resolution
QSCAT	Quick Scatterometer	0.250° × 0.250°
NOGAPS	Navy Operational Global Atmospheric Prediction System	1.000° × 1.000°
ERA-40	ECMWF 40-year Reanalysis	1.125° × 1.125°
NCEP	National Centers for Environmental Prediction	1.875° × 1.875°

[a]ERA-40 and NCEP are reanalysis products, and NOGAPS is an operational system. Basic information and further details of each data product can be found in the papers by *Liu* [2002] for QSCAT, *Rosmond et al.* [2002] for NOGAPS, *Uppala et al.* [2005] for ERA-40, and *Kanamitsu et al.* [2002] for NCEP. The NCEP product we use here is the second reanalysis. Each product has different boundary layer parameterizations and data assimilation methods. Thus, some differences in their outputs can be expected. Each data product given in Table 1 has its unique biases and limitations. ECMWF, European Centre for Medium-Range Weather Forecasts.

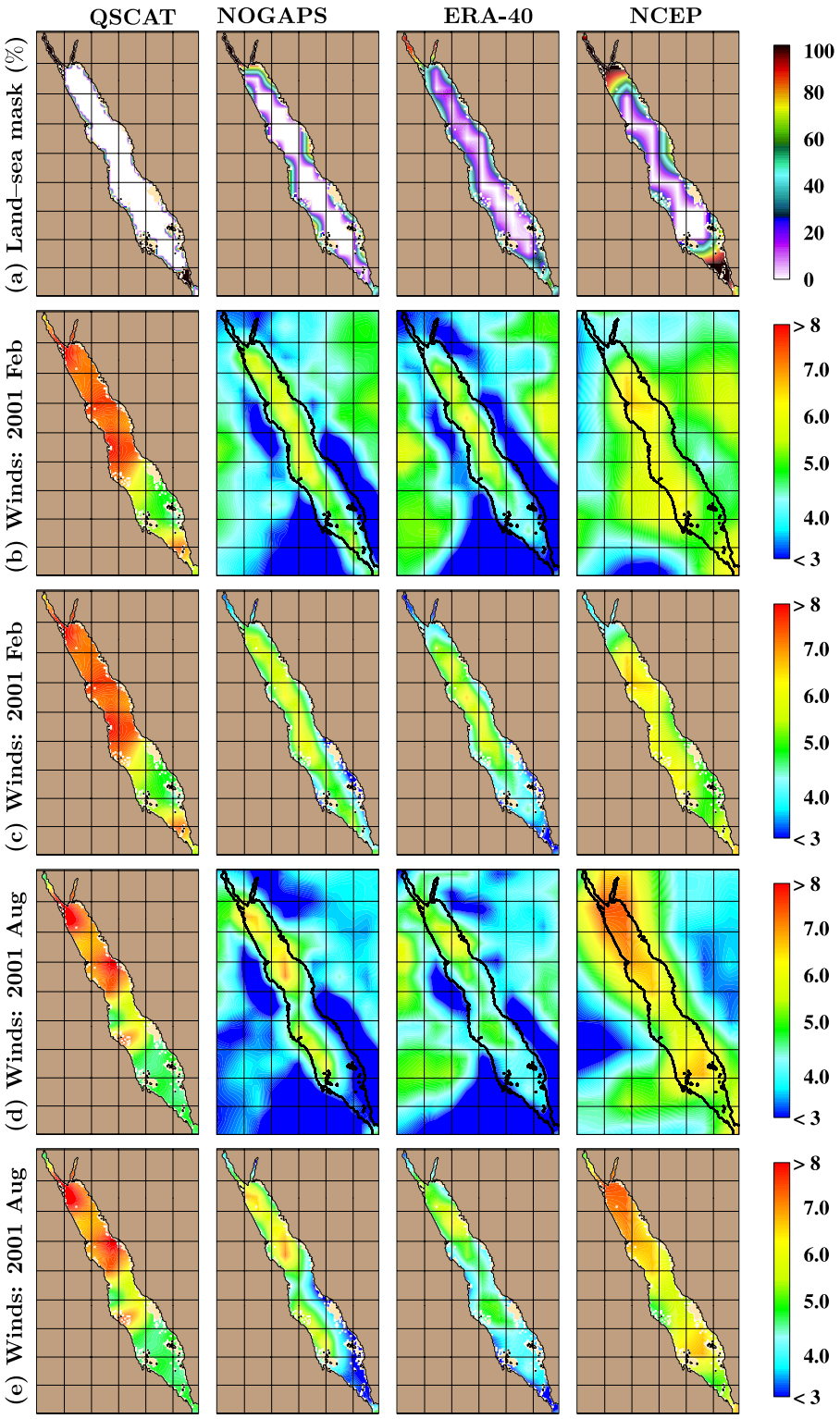

Figure 2. Land-sea masks and monthly mean of 10 m wind speeds from QSCAT, NOGAPS, ERA-40, and NCEP. (a) The land-sea mask values in percentage over the Red Sea; (b) winds over land and the Red Sea during February of 2001; (c) the same as in Figure 2b, but NWP winds are shown over the Red Sea only; (d) wind speeds over land and the Red Sea during August of 2001; and (e) the same as Figure 2d, but NWP winds are shown over the Red Sea only.

over the sea are 40% (100%) contaminated by winds over land.

[7] The land-sea mask for QSCAT has a different meaning since all satellite measurements are over the sea, and thus there is no land contamination. We describe the satellite-based QSCAT mask as 1.0 for data void areas and 0.0 for regions with valid QSCAT winds. On a month by month basis the mask could vary depending on the orbital pattern. A land-sea mask value of 1.0 for QSCAT winds indicates that there are no valid measurements in that region, in that particular month; this most commonly occurs near the coast. Note that the scatterometer cannot make reliable measurements within 35 km of the coast.

[8] In Figure 2a, the most obvious feature of the land-sea mask values is that the land contamination from NWP products exists near all coastal boundaries of the Red Sea. This is especially seen from National Centers for Environmental Prediction (NCEP), which has the coarsest grid resolution. The land-sea mask from ERA-40 also reveals lots of land contamination near the coastal boundaries with only a small white region in the interior where there is no land contamination. This indicates that sensible and latent heat flux computations presented in the paper by *Matsoukas et al.* [2007] are all based on land-contaminated wind speed values. It is emphasized that in grid cells near the coastline ERA-40 provides both land values and sea values with the final cell-averaged value based on the fraction of land. ERA-40 only has true sea-only values where its land-sea mask is exactly zero, which is far away from the coast. For all products, also including QSCAT, there is no confidence in the accuracy of wind in the northernmost end of the Red Sea on the basis of the land-sea masks because of their insufficient grid resolution.

3.2. Comparisons Against Satellite Winds

[9] Spatial variations of wind speed at 10 m from QSCAT are compared to those from NWP products during February and August of 2001 (Figures 2b, 2c, 2d, and 2e). These two months are chosen for illustrative purposes. Figure 2b is identical to Figure 2c except that the former also includes winds over land. Winds from QSCAT are available starting from July 1999 onward, but winds from the ERA-40 reanalysis are not available beyond September 2002. For comparison purposes, we therefore choose the year 2001. Satellite-based QSCAT winds are taken as truth, justified because there is no land contamination in the QSCAT winds and they are more reliable than NWP winds near the land-sea boundaries over the global ocean [*Kara et al.*, 2008a].

[10] For NWP winds in February, the consequences from land contamination are severe especially for Navy Operational Global Atmospheric Prediction System (NOGAPS) and ERA-40 (Figure 2b). Since wind speeds over land are low (e.g., <3 m s^{-1}), land contamination makes wind speed weaker over the sea near the coastal boundaries. Wind speed estimates over coastal waters are relatively weaker than those in the interior. NCEP winds over land near the coastal boundary are weak as well, but they are stronger than those from NOGAPS and ERA-40. Thus, relatively coarse resolution NCEP winds have low contrast between land and sea points. This low contrast diminishes the impact from the land contamination in NCEP. Similar features are also evident in August (Figure 2d).

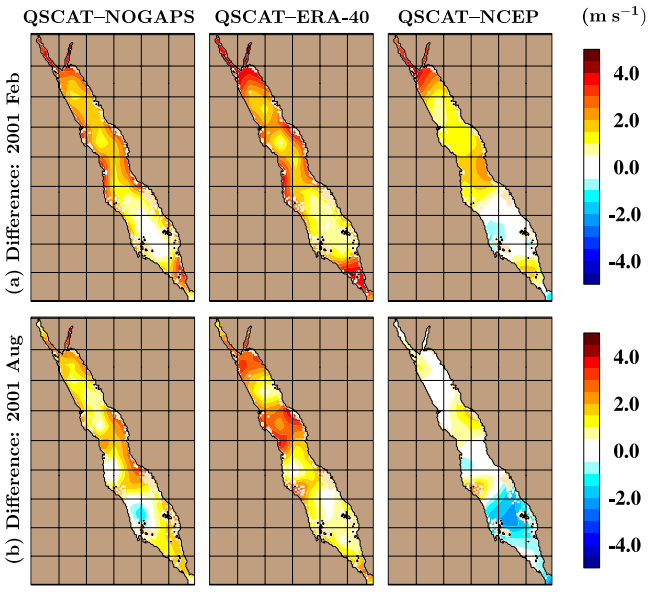

Figure 3. Differences in monthly mean wind speeds from NWP products in comparison to those from QSCAT during February and August of 2001. NWP winds are subtracted from QSCAT winds, such that differences are computed as QSCAT-NOGAPS, QSCAT-ERA-40, and QSCAT-NCEP. For the coarsest resolution NCEP, one would expect even more differences near the coastal boundaries in winds in comparison to QSCAT. However, this is noted neither in (a) February nor in (b) August. The original NCEP winds do not show a serious effect from land contamination because its winds over the land are not very different than those over the sea near the land-sea boundary.

[11] Winds from all products are generally uniform over the Red Sea during February (Figure 2c) and August (Figure 2e) of 2001. The common feature of NWP winds is that they are all weaker than the satellite-based QSCAT winds not only near the coastal boundaries but also in the interior, especially in the northern part of the region where QSCAT winds are much stronger (>2 m s^{-1}). Weaker winds from NWP products also exist in other months (not shown).

[12] Differences between NWP and QSCAT winds are computed to examine typical biases for the fields shown in Figures 2b and 2c. Winds from NWP products are almost always weaker than those from QSCAT over the Red Sea with some exceptions (Figure 3). Differences in the interior are $\approx$1 m s^{-1} and can even be larger in the case of ERA-40 during both February and August of 2001. Near the coastal boundaries of the Red Sea, differences from QSCAT are >3–4 m s^{-1}, particularly for ERA-40 winds, because of the relatively large land contamination of winds over the sea.

[13] As demonstrated above, winds from QSCAT are stronger than those from ERA-40. Here, we have a demonstration of what percentage of this is due to the resolution/land mask issue (and other regional effects) and how much is due to the fact that QSCAT winds are normally stronger the ERA-40 winds. Using a $1^\circ \times 1^\circ$ uniform grid over the Red Sea, basin average of the QSCAT wind speeds is 6.4 m s^{-1} in February of 2001. Because all QSCAT wind measurements are only over water, they are not affected by land contamination. Basin average of original wind speeds

from ERA-40 is 3.9 m s^{-1}, and this includes the effects of land contamination. The original ERA-40 winds have a 39% (1-(3.9 m s^{-1}/6.4 m s^{-1})) low bias relative to QSCAT.

[14] If one tries to exclude land contamination by using the sea-fill methodology [*Kara et al.*, 2007a], basin average of the ERA-40 wind speeds becomes 5.3 m s^{-1}, a 17% low bias relative to QSCAT. Note that the creeping sea-fill technique makes use of only over-sea values of any given scalar atmospheric variable (e.g., wind speed here) and replaces the value associated with each land-masked point by one using only nearby sea values [see also *Kara et al.*, 2008a]. In other words, wind speeds shown in the white regions of the land-sea mask of ERA-40 (see Figure 2a) are interpolated to the coastal boundaries. The program for the creeping sea-fill methodology is available online at http://www7320.nrlssc.navy.mil/nasec/. Thus, 56% (1-(17%/39%)) of the original ERA-40 low wind speed bias is due to land contamination that is remedied by the application of the creeping sea-fill in February of 2001. The remainder of the low bias is not attributable to the land contamination as it is evident in the interior of the Red Sea, i.e., even away from land, ERA-40 winds are 17% weaker than QSCAT.

4. Heat Budget in the Red and Black Seas

[15] One of the most important variables in determining the heat budgets in the Red and Black Seas is latent heat flux. As discussed in the preceding section (Figure 3), in comparison to fine resolution QSCAT, there are large errors in winds from NWP products near the coastal boundaries of the Red Sea. Because latent heat flux is a direct function of wind speed at 10 m in the bulk formulation, we examine whether the resulting heat budget can be significantly affected by ignoring the land contamination, as was done by *Matsoukas et al.* [2007]. On the basis of new calculations, updated values for the heat budget components are also provided for the Red and Black Seas.

[16] To demonstrate the impact of land contamination on latent heat flux, we compute climatological monthly means on the basis of 6 hourly outputs from ERA-40 reanalysis from 1 September 1978 to 1 September 2002 (25 years). We started from 1978 rather than 1957, when the original ERA-40 analysis started, because most of the satellite data used in the assimilation procedure became available around 1979. Climatological means are computed at two grid resolutions: $1^\circ \times 1^\circ$ grids to be consistent with *Matsoukas et al.* [2007] and $1/12^\circ \times 1/12^\circ$ grids to further include coastal regions of the Red Sea.

[17] As an example, climatological mean of latent heat flux is examined in February. In addition to original values directly obtained from ERA-40 at 1° and $1/12^\circ$ resolutions (Figures 4a and 4c), we also show sea-filled latent heat fluxes for the corresponding fields (Figures 4b and 4d) after the creeping sea-fill methodology described earlier is applied. The land contamination is so severe near the coastal boundaries of the Red Sea that values of latent heat fluxes that had been exceedingly low (e.g., 50 W m^{-2}) become very high (e.g., 200 W m^{-2}) after the creeping sea-fill, especially in the northernmost areas. Excessively low latent heat fluxes from the original ERA-40 reanalysis can easily be attributed to unrealistically weak winds from ERA-40 (Figure 3a). The creeping sea-fill reduces land contamination from latent heat fluxes at both grid resolutions (Figures 4b and 4d).

[18] The importance of using a fine resolution ocean grid of $1/12^\circ$ as opposed to a coarse grid of 1° in obtaining basin-averaged latent heat fluxes is evident in Table 2. Although original ERA-40 values can be quite different, sea-filled values agree with each other quite well. Annually, differences between original and and sea-filled latent heat flux values can be as large as 50 W m^{-2}. *Matsoukas et al.* [2007] do not have any specific consideration for the land contamination. As expected, such contamination from the 1° gridded field is relatively large. While it is not shown here, land contamination of radiation fluxes is less severe (<30 W m^{-2}).

[19] One may notice that the sea-filled latent heat climatologies look different from original fields calculated from ERA-40 (Figure 4). This can be explained as follows. On the basis of the land-sea mask of ERA-40 (Figure 2a) there is essentially one single ERA-40 sea value for each of its latitude bands in the Red Sea, and a few bands have two values). This means that the across the sea variation in ERA-40 is entirely from land/sea differences. Using the sea-fill approach, we assume the land is like the closest sea point. Therefore, there is no across the sea variation in this case. This is clearly seen in the plot south of 22°N. North of 22°N, one sees some across the sea variation (where ERA-40 has two grid points over sea). However, the sea grid points are also much more consistent (blue) and significantly different from the nearby land points. The blue values are in the all-values plots, but swamped by other color contours from land. The impact of land contamination due to coarse grid resolutions of NWP products is also discussed in the Black Sea [*Kara et al.*, 2008b].

[20] Finally, for completeness we present net heat budgets for the Red and Black Seas (Table 3). For each component of the net heat budget, sea-filled values are first produced on the basis of the land-sea mask of ERA-40 (Figure 2a). Climatological means are then computed on the basis of 6 hourly values during 1978–2002. It is quite remarkable that when using the sea-filled ERA-40 data, the heat budget is successfully closed in the Black Sea with a net value of 0 W m^{-2}. The heat budget in the Red Sea is also almost closed with a net value of -8 W m^{-2}.

5. Additional Comments

[21] In this commentary, so far our major focus has been on the land contamination issues, resulting in improper estimates of the heat budget in the Red and Black Seas. There are two more additional points. First important isssue is that all results presented in the paper by *Matsoukas et al.* [2007] are derived using monthly means of atmospheric variables to compute monthly mean latent and sensible heat fluxes. In traditional climate studies [e.g., *Josey et al.*, 1999; *Boyer et al.*, 2006], high-frequency observations of wind speed and other atmospheric variables are used to make estimates of heat flux which are then averaged to compute monthly means. *Matsoukas et al.* [2007] could have used the 6 hourly NWP products to estimate 6 hourly latent and sensible heats fluxes from which monthly means could be calculated. Using monthly mean atmospheric variables in computing "monthly" fluxes can result in ≈20% difference

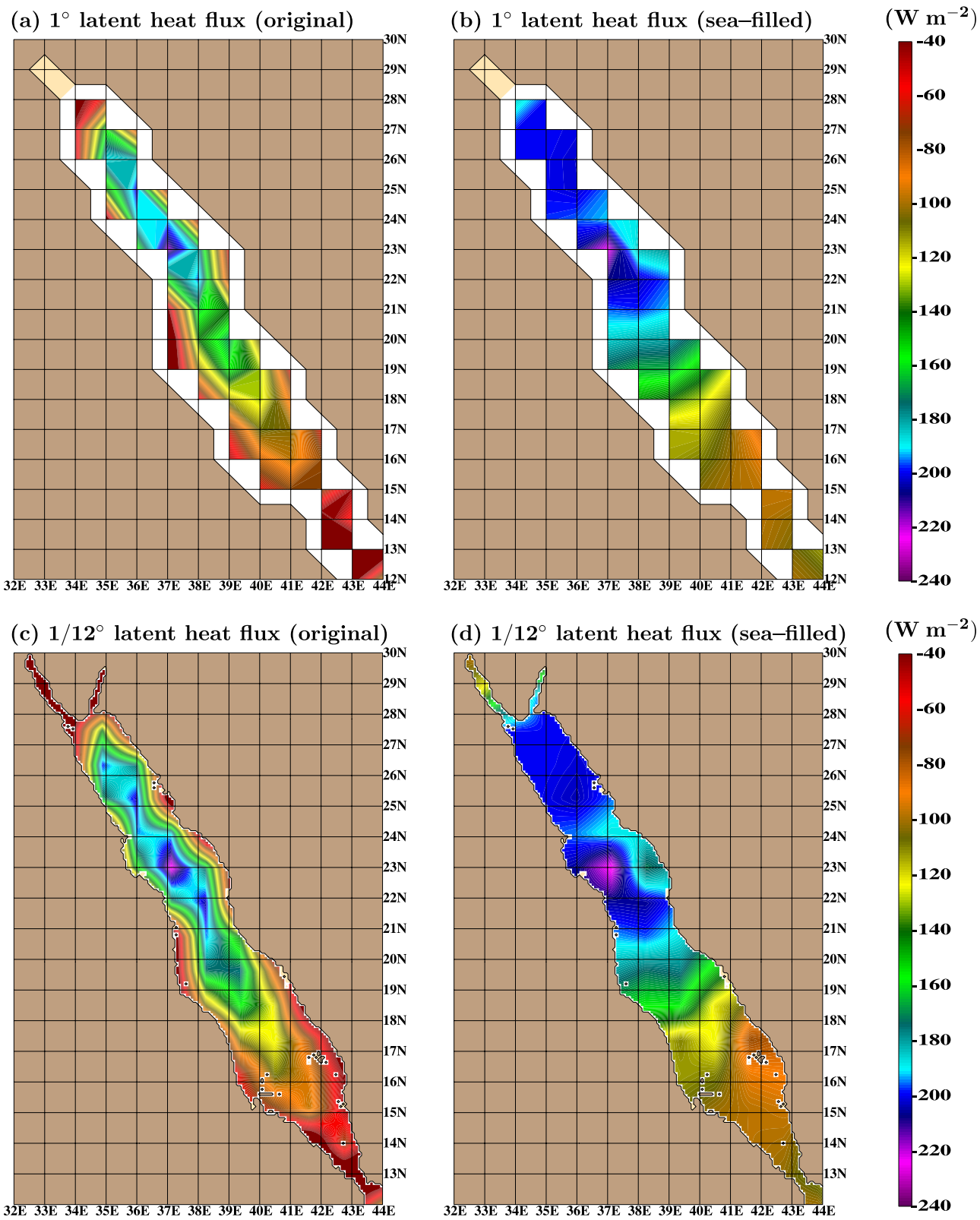

Figure 4. Climatological mean of latent heat flux values in February before and after the creeping sea-fill is applied. Monthy means are based on 6 hourly outputs of ERA-40 output during 1978–2002. (a, b) The white space indicates the extent of sea points at 1° × 1° resolution.

Table 2. Basin-Averaged Latent Heat Flux Values Before and After the Creeping Sea-Fill in the Red Sea[a]

	1° Latent Heat Flux (W m^{-2})			1/12° Latent Heat Flux (W m^{-2})		
Month	Original	Sea-Filled	Difference	Original	Sea-Filled	Difference
Jan	−92	−169	−77	−126	−172	−46
Feb	−83	−152	−69	−114	−156	−42
Mar	−67	−118	−51	−90	−122	−32
Apr	−51	−85	−34	−66	−87	−21
May	−48	−80	−32	−62	−82	−20
Jun	−55	−95	−40	−75	−98	−23
Jul	−58	−98	−40	−79	−101	−22
Aug	−63	−106	−43	−84	−109	−25
Sep	−61	−105	−44	−81	−107	−26
Oct	−70	−124	−54	−92	−124	−32
Nov	−88	−161	−73	−120	−163	−43
Dec	−92	−170	−78	−126	−173	−47
Annual	−69	−122	−53	−93	−125	−32

[a]Climatological monthly mean of latent heat flux is calculated using 6-hourly outputs from ERA-40 reanalysis during 1978–2002. This is done for both original and sea-filled latent heat flux values. The creeping sea-fill methodology is described in the text. Differences are obtained by subtracting original ERA-40 latent heat flux values from those obtained after the creeping sea-fill. Climatological long-term annual mean over all months is given in the last row. Standard deviations of monthly mean values typically vary between 20 W m^{-2} and 50 W m^{-2}. Standard deviation values averaged over the annual cycle are 45 (25 W m^{-2}) for the 1° original (sea-filled) latent heat fluxes and 34 (25 W m^{-2}) for the 1/12° original (sea-filled) latent heat fluxes.

depending on the time and location [e.g., *Lee et al.*, 2005; *Gulev*, 1997].

[22] Another fundamental problem in the paper by *Matsoukas et al.* [2007] is that in computing latent and sensible heat fluxes they use outdated parameterizations for exchange coefficients [*Vardavas*, 1987]. Their study assumes neutral atmospheric conditions for each month, and the above mentioned monthly winds are preferred in these calculations. However, there has been significant progress in determining exchange coefficients since 1987. For example, the well-known and commonly used Couped Ocean-Atmosphere Response Experiment (COARE) algorithm (v3.0) provides up-to-date exchange coefficient parameterizations for computing latent and sensible heat fluxes [*Fairall et al.*, 2003]. Results based on the COARE algorithm clearly reveal that ignoring the effects of vapor mixing ratio in the parameterization of exchange coefficient can give a flux value that is ≈3–5 times less than its actual value at very low wind speeds [*Kara et al.*, 2005]. This is further illustrated at the web page http://www7320.nrlssc.navy.mil/nasec/. Using only wind speed and ignoring air-sea stratification (i.e., neutral case) can also cause errors as large as 20% or more in the wind stress exchange coefficient even on monthly means [*Kara et al.*, 2007b].

6. Summary and Conclusions

[23] Results presented by *Matsoukas et al.* [2007] ignore land contamination in obtaining the heat budget for the Red and Black Seas. We demonstrate that near coastal boundaries, the spatially coarse NWP products have errors not only in the wind fields. Because of large errors (>3 m s^{-1}) in ERA-40 winds, corrections to winds are essential in the heat budget computations. Postprocessing of winds and other NWP fields can reduce errors in latent and sensible heat fluxes near the land-sea boundaries. We found that ignoring the land contamination on latent heat fluxes could result in basin-averaged errors as high as 50 W m^{-2}, significantly changing the heat budget. The errors near the coastline can often be >100 W m^{-2}. As it is demonstrated in this paper, sea-filled shortwave and longwave radiation values processed from ERA-40 and interpolated to fine resolution ocean grids (1/12°) are sufficiently accurate since the net surface heat budget is almost closed in both regions.

[24] One of the main goals of their study is to demonstrate that the energy balance method disagrees with the bulk aerodynamic approach. However, the wind errors in their application of the bulk formulation make it difficult to justify comparison between the two methodologies. Specifically, some values of heat budget components presented by *Matsoukas et al.* [2007] are somewhat consistent with ours shown in Table 3 but this appears to result from a cancellation of errors. For example, by using improper exchange coefficients they may have obtained relatively higher latent and sensible heat fluxes. The use of land-contaminated winds will lead to low estimates of latent heat flux. Errors in other terms would have to compensate by inflating the latent heat flux. In addition, monthly mean winds used for computing monthly mean heat fluxes would lead to additional errors in

Table 3. Basin-Averaged Values of Climatological Mean of Heat Budget Components for the Red and Black Seas[a]

	Shortwave	Longwave	Latent	Sensible	Total
		Red Sea			
Jan	147	−91	−172	−15	−131
Feb	182	−96	−156	−11	−81
Mar	220	−95	−122	−3	0
Apr	247	−94	−87	3	69
May	259	−97	−82	5	85
Jun	266	−106	−98	9	71
Jul	257	−96	−101	9	69
Aug	246	−92	−109	7	52
Sep	229	−96	−107	3	29
Oct	199	−97	−124	−2	−24
Nov	162	−94	−163	−7	−102
Dec	141	−91	−173	−13	−136
Annual	213	−95	−125	−1	−8
		Black Sea			
Jan	43	−58	−57	−25	−97
Feb	75	−61	−50	−21	−57
Mar	125	−59	−33	−8	25
Apr	181	−59	−19	2	105
May	227	−65	−25	0	137
Jun	243	−68	−47	−2	126
Jul	238	−69	−69	−3	97
Aug	204	−71	−94	−6	33
Sep	151	−74	−101	−13	−37
Oct	93	−70	−91	−20	−88
Nov	51	−64	−79	−27	−119
Dec	34	−58	−66	−27	−117
Annual	139	−65	−61	−13	0

[a]Values are given in W m^{-2}. The net surface energy balance is expressed as the sum of the downward surface solar irradiance, upward longwave radiation, and the downward latent and sensible heat fluxes (Q_L and Q_S). Monthly mean value is obtained after interpolating each component of net surface heat flux at every 6 hour time interval to the 1/12° grid by using the creeping sea-fill to reduce land contamination. All results are based on the ERA-40 data set during 1978–2002. Climatological long-term mean over all months is given in the last row. Standard deviation values averaged over the annual cycle are 12, 16, 25, and 5 W m^{-2} for shortwave radiation, longwave radiation, latent heat flux and sensible heat fluxes for the Red Sea. Similarly, they are 8, 4, 9, and 4 W m^{-2} for the Black Sea.

the resulting heat budget. Our estimates are also based on slightly longer time period of 1978–2001.

[25] Satellite-based QSCAT winds can be used for estimating heat budgets in the future. While the available time period of 1999 onward for QSCAT winds may not be long enough for climatological studies, such a fine resolution gridded (0.25°) product would provide spatial resolution more appropriate for the narrow Red and Black Seas. In addition, land contamination in atmospheric variables needs to be taken into consideration whenever NWP products are used for computing heat budgets over sea-only locations.

[26] **Acknowledgments.** A. Wallcraft of NRL is greatly appreciated for his helpful comments. The authors acknowledge the invaluable suggestions provided by the reviewer. Additional thanks go to C. Matsoukas for numerous discussions. This work is funded by the Office of Naval Research (ONR) under the 6.2 project, Improved Synthetic Ocean Profiles (ISOP). The paper is contribution NRL/JA/7320/08/8084 and has been approved for public release.

References

Boyer, T. P., J. I. Antonov, H. E. Garcia, D. R. Johnson, R. A. Locarnini, A. V. Mishonov, M. T. Pitcher, O. K. Baranova, and I. V. Smolyar (2006), *World Ocean Database 2005* [DVD], *NOAA Atlas NESDIS*, vol. 60, edited by S. Levitus, 190 pp., NOAA, Silver Spring, Md.

Fairall, C. W., E. F. Bradley, J. E. Hare, A. A. Grachev, and J. B. Edson (2003), Bulk parameterization of air-sea fluxes: Updates and verification for the COARE algorithm, *J. Clim.*, *16*, 571–591.

Gulev, S. K. (1997), Climatologically significant effects of space-time averaging in the North Atlantic sea-air heat flux fields, *J. Clim.*, *10*, 2743–2763.

Josey, S. A., E. C. Kent, and P. K. Taylor (1999), New insights into the ocean heat budget closure problem from analysis of the SOC air-sea flux climatology, *J. Clim.*, *12*, 2856–2880.

Kanamitsu, M., W. Ebisuzaki, J. Woollen, S.-K. Yang, J. J. Hnilo, M. Fiorino, and G. L. Potter (2002), NCEP-DOE AMIP-II reanalysis (R-2), *Bull. Am. Meteorol. Soc.*, *83*, 1631–1643.

Kara, A. B., H. E. Hurlburt, and A. J. Wallcraft (2005), Stability-dependent exchange coefficients for air-sea fluxes, *J. Atmos. Oceanic Technol.*, *22*, 1080–1094.

Kara, A. B., A. J. Wallcraft, and H. E. Hurlburt (2007a), A correction for land contamination of atmospheric variables near land-sea boundaries, *J. Phys. Oceanogr.*, *37*, 803–818.

Kara, A. B., A. J. Wallcraft, E. J. Metzger, H. E. Hurlburt, and C. W. Fairall (2007b), Wind stress drag coefficient over the global ocean, *J. Clim.*, *20*, 5856–5864.

Kara, A. B., A. J. Wallcraft, C. N. Barron, H. E. Hurlburt, and M. A. Bourassa (2008a), Accuracy of 10 m winds from satellites and NWP products near land-sea boundaries, *J. Geophys. Res.*, *113*, C10020, doi:10.1029/2007JC004516.

Kara, A. B., C. N. Barron, A. J. Wallcraft, T. Oguz, and K. S. Casey (2008b), Advantages of fine resolution SSTs for small ocean basins: Evaluation in the Black Sea, *J. Geophys. Res.*, *113*, C08013, doi:10.1029/2007JC004569.

Lee, S.-K., D. B. Enfield, and C. Wang (2005), Ocean general circulation model sensitivity experiments on the annual cycle of Western Hemisphere Warm Pool, *J. Geophys. Res.*, *110*, C09004, doi:10.1029/2004JC002640.

Liu, W. T. (2002), Progress in scatterometer application, *J. Oceanogr.*, *58*, 121–136.

Matsoukas, C., A. C. Banks, K. G. Pavlakis, N. Hatzianastassiou, P. W. Stackhouse Jr., and I. Vardavas (2007), Seasonal heat budgets of the Red and Black seas, *J. Geophys. Res.*, *112*, C10017, doi:10.1029/2006JC003849.

Rosmond, T. E., J. Teixeira, M. Peng, T. F. Hogan, and R. Pauley (2002), Navy Operational Global Atmospheric Prediction System (NOGAPS): Forcing for ocean models, *Oceanography*, *15*, 99–108.

Uppala, S., et al. (2005), The ERA-40 re-analysis, *Q. J. R. Meteorol. Soc.*, *131*, 2961–3012, doi:10.1256/qj.04.176.

Vardavas, I. M. (1987), Modelling the seasonal variation of net all-wave radiation flux and evaporation in a tropical wet-dry region, *Ecol. Modell.*, *39*, 247–268.

C. N. Barron and A. B. Kara, Oceanography Division, Naval Research Laboratory, Stennis Space Center, Code 7320, Building 1009, MS 39529, USA. (birol.kara@nrlssc.navy.mil)